land

MDPI

Article

Long-Term Monitoring of Trends in Xerothermality and Vegetation Condition of a Northeast Mediterranean Island Using Meteorological and Remote Sensing Data

Panteleimon Xofis [1,*], Elissavet Feloni [2], Dimitrios Emmanouloudis [1,3], Stavros Chatzigiovanakis [1], Kalliopi Kravari [3], Elena Samourkasidou [3], George Kefalas [4] and Panagiotis Nastos [5]

[1] Department of Forestry and Natural Environment Sciences, Democritus University of Thrace, 1st km Drama-Mikrohori, GR66100 Drama, Greece; demmano@neclir.duth.gr (D.E.); schatzig@neclir.duth.gr (S.C.)
[2] Department of Surveying and Geoinformatics Engineering, Egaleo Park Campus, University of West Attica, 5 Ag. Spyridonos Str., GR12243 Athens, Greece; efeloni@uniwa.gr
[3] ASSIST Lab (Analysis and Management of Natural Disasters and Technological Risks), Democritus University of Thrace, 1st km Drama-Mikrohori, GR66100 Drama, Greece; kkravari@ihu.gr (K.K.); esamourk@arch.duth.gr (E.S.)
[4] Department of Geography, Harokopio University, El. Venizelou 70, Kallithea, GR17676 Athens, Greece; gkefalas@hua.gr
[5] Laboratory of Climatology and Atmospheric Environment, Department of Geology and Geoenvironment, National and Kapodistrian University of Athens, University Campus, GR15784 Athens, Greece; nastos@geol.uoa.gr
* Correspondence: pxofis@neclir.duth.gr; Tel.: +30-6973035416 or +30-2521060430

Abstract: There is no doubt that global climate change is happening and affecting life on Earth in a variety of ways. It can be seen on the extreme events of natural disasters, prolonged periods of drought, and increased summer and annual temperatures. While climate change affects every place on Earth, the Mediterranean region is considered a hot spot of climate change. Temperature is expected to increase further, precipitation, especially during summer months, is expected to decrease, and extreme rainfall events are projected to increase. These projected changes will affect both continental and insular environments, with small islands being particularly vulnerable due to the lack of space for species to move into more favorable conditions. As a result, these environments need to be studied, the changes quantified, and the consequences monitored. The current study focuses on the island of Fournoi in the central eastern part of the Aegean Sea. We employed data from a local meteorological station, which operates for a limited period, the Climate Research Unit TS data, and remote sensing thermal data to monitor the trends in aridity over a period of almost 40 years. The results show that summer temperature has increased significantly over the last 40 years, and this is confirmed by both meteorological and remote sensing data. At the same time, precipitation seems to remain stable. Despite the increased aridity imposed by the increased temperature and stable precipitation, vegetation seems not to be experiencing extreme stress. On the contrary, it seems to be following a positive trend over the study period. This observation is explained by the extreme resilience of the plant species of the study area and the fact that vegetation has been recovering over the last 50 years after a period of human overexploitation, and this recovery overcomes the stress imposed by increased aridity.

Keywords: vegetation condition index; temperature condition index; Landsat; CRU TS; NDVI; LST; small islands; drought; aridity

check for updates

Citation: Xofis, P.; Feloni, E.; Emmanouloudis, D.; Chatzigiovanakis, S.; Kravari, K.; Samourkasidou, E.; Kefalas, G.; Nastos, P. Long-Term Monitoring of Trends in Xerothermality and Vegetation Condition of a Northeast Mediterranean Island Using Meteorological and Remote Sensing Data. *Land* **2024**, *13*, 2129. https://doi.org/10.3390/land13122129

Academic Editors: Paulette Posen, Naomi Greenwood, Michelle Devlin and Carlos Campos

Received: 18 October 2024
Revised: 4 December 2024
Accepted: 6 December 2024
Published: 8 December 2024

Copyright: © 2024 by the authors. Licensee MDPI, Basel, Switzerland. This article is an open access article distributed under the terms and conditions of the Creative Commons Attribution (CC BY) license (https://creativecommons.org/licenses/by/4.0/).

1. Introduction

The complex geological history and topography of the Mediterranean basin, climatic changes prior to and after the establishment of the Mediterranean climate, approximately 3 million years ago [1], and the patchwork of ecological niches and habitats have all resulted

in a very rich biodiversity, including many endemic species making the Mediterranean basin one of the global biodiversity hotspots [2–7]. This high biodiversity is a characteristic of all Mediterranean regions, and, although they occupy only 5% of the Earth's surface, they harbor 20% of the known vascular plants of the world [8]. In the Mediterranean basin, approximately 25,000 plant species exist within an area of 2.3 million km^2 [9]. If this number is compared with the 6000 species that exist in non-Mediterranean Europe in an area of 9 million km^2, or with the 1400 species that exist in the British Isles in an area of 308,000 km^2, then the floristic wealth of the Mediterranean basin becomes more impressive [10,11]. However, if the scale of estimation is confined to a unit of one km^2, then the species richness of the Mediterranean basin is rather low compared with the other four areas where Mediterranean ecosystems occur [3]. Of particular importance, especially from a biodiversity conservation point of view, is the number of endemic species in the Mediterranean basin. According to Blondel and Aronson [3], more than half of the plant species of the area are endemics, and Gomez-Campo [9] noted that four out of five endemic species in Europe exist in the Mediterranean basin. Finally, more than 100 tree species are present in the area as opposed to no more than 30 in Central Europe [4].

The Mediterranean islands significantly contribute to the development and maintenance of the high biodiversity of the Mediterranean basin and the high degree of endemism, and they also constitute natural laboratories of the evolutionary processes available for study and exploration [12–14]. There are more than 11,000 islands and islets in the Mediterranean basin, of which approximately 250 are regularly inhabited, making the area one of the regions with the most islands and archipelagos of the world [6]. The geographic isolation, environmental heterogeneity, and long-term human presence that characterize the Mediterranean islands have all contributed to their high biodiversity and ecological importance [6,15–17]. Over the last few decades, insular environments are subject to significant environmental and socioeconomic changes, including changes in land use patterns, fluctuations in human populations, and economic transformations that alter the traditional regime and interaction between humans and the environment [16,18–22]. At the same time, it has to be acknowledged that insular environments are particularly vulnerable and less resilient to environmental changes compared to mainland regions for a number of reasons including their geographic isolation and their relatively small area [5,17,23]. While invasive alien species, natural disasters, and increased human disturbance can all be considered significant threats to the sustainability of the insular Mediterranean Europe [12], climate change and the subsequent changes in temperature and precipitation patterns constitute probably the most significant threat for the biodiversity and sustainability of the Mediterranean islands [23].

Climate change is a global-scale phenomenon that affects the various parts of the world in different ways and intensities [24]. It can be witnessed in a number of indicators, such as the increases in air and seawater temperature, the rise in sea level, the shorter lasting of snow on the mountains, increased drought and aridity, the increased frequency of extreme natural disasters, such as wildfires and floods, and the loss of biodiversity [24–29]. The Mediterranean basin constitutes a climate change hotspot; it is negatively affected and will continue to be negatively affected by climate change in a much higher intensity than other parts of the globe [5,30]. Climate change is expected to affect ecosystem integrity, water scarcity, human health, and the quality of life as well as many other social, economic, and environmental aspects. The projected impacts are expected to be much more intense in insular environments and especially in small islands and islets [5,23]. For instance, a rise in the air temperature of 3 °C is expected to lead to an upwards movement of vegetation zones of 543 m [5]. On small islands, there is simply not enough space for the ecosystems to move upwards. Furthermore, if one considers that water scarcity is more intense in insular environments, then the increased vulnerability of these ecological laboratories to climate change becomes obvious [5,23].

Over the last 20–30 years, climate-change-driven alterations in precipitation patterns and the positive trends in temperatures [31–33] have intensified drought phenomena in

the Eastern Mediterranean region. Studies have reported a significant decline in rainfall across the region, with prolonged dry seasons and increased xerothermic conditions that exacerbate water scarcity and soil degradation. As reported by Guiot and Gramer [34], these changes have a significant impact on vegetation, particularly on insular environments, which are characterized by limited local water resources and geographic isolation, while several human-made activities, including deforestation and agricultural expansion, increase the vegetation stress. The adaptation of the environment to these pressures has led to the dominance of more drought-resistant types, such as phrygana and maquis, which exhibit significant resilience to arid conditions [4], a state that also reflects the ecological degradation taking place in the region. Hence, a deeper understanding of the link between environmental impacts and climate change is critical, and this study aims to illustrate the complex relationship between climate factors inducing droughts and vegetation condition in the Eastern Mediterranean.

Monitoring the consequences and trends of climate change is of particular importance for maintaining long-term sustainability because constant and effective monitoring can prevent detrimental interactions between combined pressures such as increased drought, increased grazing, and threat from wildfires. Remote sensing data and methods constitute a significant tool for long-term and effective monitoring of various environmental parameters, such as land use changes [35–37], landscape structure and composition [16,18–20,38], drought [39–44], and vegetation dynamics [45,46].

In the current study, we employ remote sensing data and methods, as well as local and global weather data, aiming to investigate the trends in basic climatic parameters, in xerothermality, and in vegetation condition over a period of approximately 40 years on a northeast Mediterranean island. The term xerothermality is adopted in the current study, as opposed to similar terms like aridity or drought. It describes the climatic conditions characterized by the combination of high temperature and low humidity and moisture; as a result, it reflects better the conditions analyzed in the current study. The term vegetation condition, which is employed in the current study, refers to the health and vigor of vegetation. If the aridity and drought of the area is increasing during the study period, this is expected to have a negative impact on the health and vigor of vegetation, which is expected to be detected by the employed vegetation index. The specific objectives of the study are (a) to generate a long-term database of air temperature and precipitation data by integrating local and global weather data to investigate the observed trends, (b) to investigate the trends in summer xerothermality over a period of almost 40 years using remote sensing data, and (c) to investigate the trends in vegetation condition over the same period. We believe that the methods and results of the present study will provide useful insights into the climate-change-induced trends in weather patterns, drought, vegetation, and water dynamics and will be useful to policymakers for setting short and long-term objectives for the sustainability of the Mediterranean islands. Furthermore, we believe the methodological approach presented in the current study will allow the large-scale investigation of long-term trends in drought and aridity.

2. Materials and Methods

2.1. Study Area

The study is conducted on the island complex of Fournoi Korseon, which is located in Central-East Aegean Sea (26.493740° E, 37.568441° N). Fournoi Korseon or Fournoi Ikarias or Fournoi is a cluster of 52 islands and rocky islets where the largest of them is the island of Fournoi, with an area of 2995 hectares, followed by Thymaina Island, with an area of 1002 hectares, and Agios Minas Island with an area of 219 hectares. The total area of the complex is 4484 hectares, while its total coastline is 162 km, of which 87 km are on the island of Fournoi, 30 km are on the island of Thymaina, and 16 km are on the island of Agios Minas (Figure 1). The permanent population of the complex is 1343 inhabitants, with the great majority of them in Fournoi, while the population almost doubles during

the summer period. The climate is typical Mediterranean with mild winters and hot and dry summers.

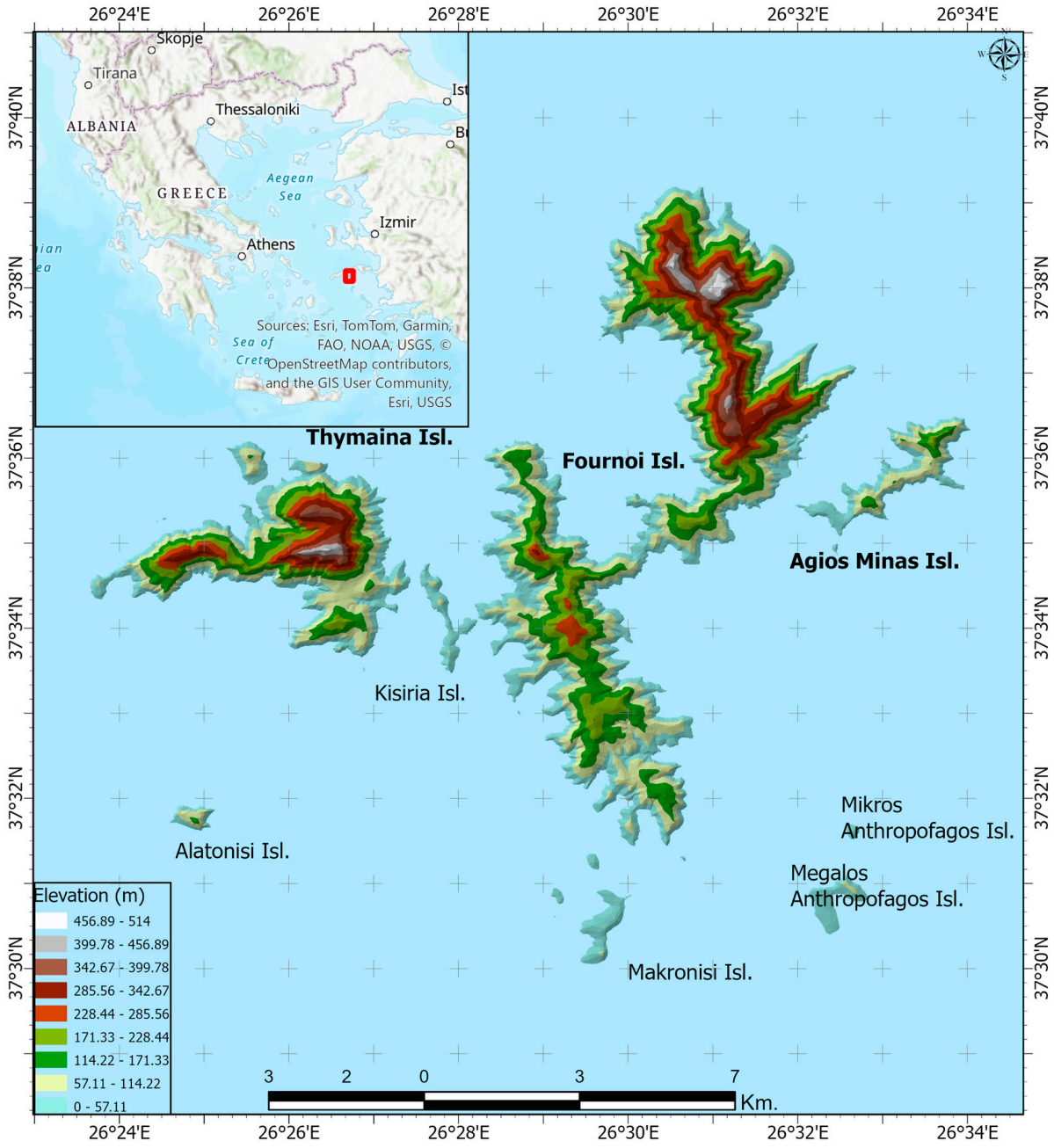


Figure 1. Study area location and geomorphology.

The area is characterized by a particularly sharp relief, which explains its long coastline, while its altitudinal variation is from sea level to the altitude of 514 m at Korakas Peak at the northern end of Fournoi Island. The sharp relief is also reflected in the fact that 83% of the area has a slope exceeding 30%. At the same time, only 3.7% of the area has slopes below 15%, where it can be used seamlessly for arable agricultural crops. So, the main land use can only be livestock farming as long as it does not threaten the ecosystems of the area. This sharp relief is expected to generate a diverse mosaic of microhabitats in terms of drought conditions and soil water availability, which in turn is expected to affect the vegetation. However, it was beyond the scope of the study to investigate the spatial variation in drought across the islands and in relation to the current mosaic of

microhabitats. Geologically, the area is dominated by schists, while in a few places the presence of limestone was observed in the field survey. Approximately, 46.5% of the area is dominated by greenschists, while 53.5% is dominated by chloritic, marly, and quartzose schists, often with layers of marbles.

The geographical position of the complex, its proximity to the Asian continent, its relative geographical isolation, and its position in the Aegean archipelago make the area a valuable ecological environment. The entire study area is a designated NATURA 2000 site, with two protection regimes. It is part of the Special Protection Area (SPA) with the name "Nisos Fournoi kai Nisides Thymaina, Alatonisi, Thymainaki, Strongylo, Plaka, Makronisi, Mikros kai Megalos Anthropofagos, Agios Minas kai Thalassia Periochi (GR4120006)" for the protection of birds under the Birds Directive (79/409/EEC), as updated by Directive 2009/147/EC. According to the special description (Standard Data Form) of the NATURA 2000 network, it is an important area for the reproduction of seabirds and species of typical Mediterranean ecosystems.

The entire area is also part of the Special Area of Conservation (SAC) site named Site of Community Importance (SCI) named "Ikaria-Fournoi kai Paraktia Zoni" (GR4120004) for the protection of habitats in accordance with the directive 92/43/EEC. According to the special description (Standard Data Form) of the NATURA 2000 network, the main element of the quality and importance of the site is its high biodiversity, which is reflected in the variety of habitat types and the abundance of endemic and locally endemic plants and invertebrates. This high degree of endemism (e.g., species endemic to the Eastern Aegean, such as *Cephalaria squamiflora* ssp. *Squaliform,* and *Onopordum majorii*) results mainly from the geographical location (very close to Asia Minor), the complex geomorphology, and the variety of habitats present.

In the area, there are 12 habitat types of Annex II of the Directive 92/43/EEC (Figure 2). The dominant one is "Arborescent matorral with *Juniperus* spp.—5210", occupying 44.45% of the area, while the Juniper species that characterizes the habitat is *Juniperus phoenicea* L. 1753. This habitat type probably constitutes the climax vegetation type of the area, while field observation revealed that the habitat appears generally degraded. According to Tsiourlis et al. [47], this vegetation type in the study area is classified in the *Pistacio—Juniperetum phoeniceae Trinajstić* 1987 community and in the *Pistacio—Juniperetum phoeniceae Rhamnietosum lycioides* subcommunity. It is characterized by the presence of extremely thermophilic and xerophilic species, such as *Rhamnus lycioides*, *Micromeria nervosa*, *Asphodelus ramosus,* and *Muscari comosum*. In the Eastern Aegean islands, due to their proximity to the Turkish peninsula, there is a large number of herbaceous species, including *Briza maxima*, *Trifolium campestre*, *Trifolium stellatum*, *Verbascum cylindrocarpum*, *Hypochaeris achyrophorus*, *Brachypodium distachyon*, *Catapodium rigidum*, etc., which are also all adapted to arid conditions. A significant part of the area (36.95%) is occupied by the habitat type "*Sarcopoterium spinosum* phryganas—5420", which constitutes the typical Phryganic vegetation type of the area, as well as of many islands of central and southern Aegean. Apart from *Sarcopoterium spinosum*, which is the dominant species for this vegetation type, other species such as *Genista acanthoclada*, *Thymus capitatus*, *Anthylis hermania*, *Cistus* spp., *Erica verticilata,* etc., are also present. According to Tsiourlis et al. [48], the *Sarcopterium spinosum* communities of the Aegean islands are classified in the *Sarcopoterietum spinosi* Zohary 1947 community. For this exact study area, the authors identify the subcommunity *Sarcopoterietum spinosi micromerio-hypericetosum empetrifolium* as the most likely to occur. This specific subcommunity seems to be typical of the islands of the Eastern Aegean that receive the influence of the Eastern warm current and are also characterized by particularly mild winters and very hot summers. The habitat type "Vegetated sea cliffs of the Mediterranean coasts with endemic *Limonium* spp.—1240" occupies approximately 6% of the area, and human land uses (code 10) is 6.67%. The rest of the habitat types found in the study area are much more limited with a coverage not exceeding 3%.

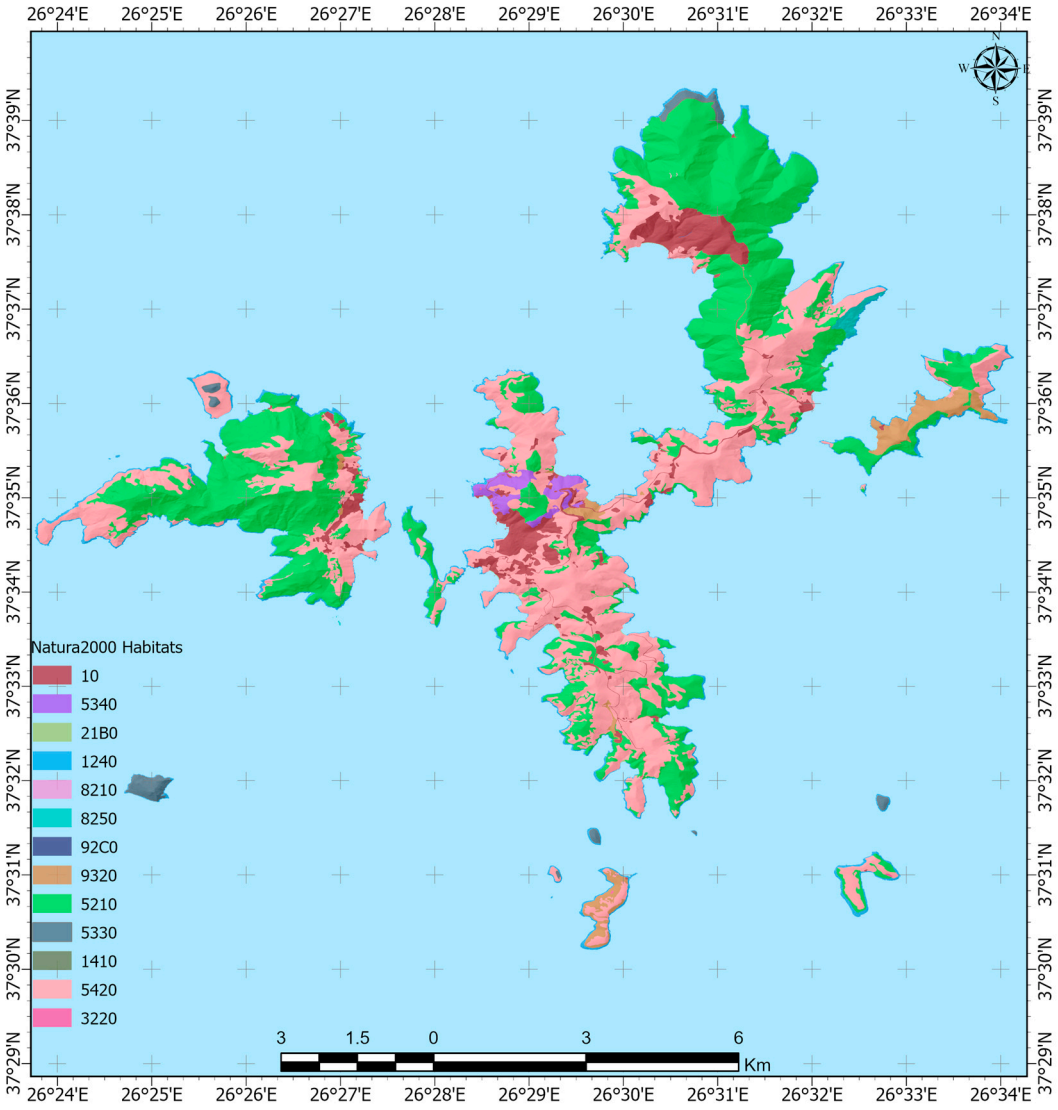


Figure 2. Distribution of Natura2000 Habitats in the study area.

2.2. Methodological Approach

Multiple data have been employed in the current study, including data derived from both in situ measurements of climate parameters and climate parameters derived from Climatic Research Unit gridded Time Series (CRU TS; [49]), as well as time series analysis of satellite images. Field measurements were collected from the meteorological station (MS) of the Meteo network, which is installed at an altitude of five meters with coordinates 37.577412° N and 26.479984° E [50]. These data cover the period from July 2012 to December 2021 and include daily average, maximum and minimum temperature, daily average, maximum and minimum relative humidity, and daily precipitation. The specific time period covered is considered rather short to draw definitive conclusions about the trends of xerothermality in the study area. However, they formed a valuable dataset, which was used in multiple ways as is described in the following paragraphs.

The locally collected data were initially used for the creation of the Bagnouls Gaussen Climatic Diagram of the study area based on these data. The second and very important use of the local data was their combined analysis with CRU TS data, which cover a much longer time period, starting from the beginning of the 20th century. The CRU TS data are a product of the spatial interpolation of data collected from stations located at a distance, which sometimes is quite far away from the area of interest. The spatial interpolation method employed for the generation of this global scale dataset is the angular-distance

weighting (ADW) [49]. According to the data developers, this spatial interpolation method improved the quality of the produced data, and it "*provides improved traceability between each gridded value and the input observations, and allows more informative diagnostics that dataset users can utilise to assess how dataset quality might vary geographically*". Of course, the fact that they are a product of spatial interpolation and not in situ measurements leads to a relative uncertainty regarding their accuracy, compared to actual locally collected data. For this reason, these data were used in combination with the actual data of the period 2012–2021 to build a model that corrects the CRU TS data based on the actual on-site data. The method adopted is that of linear regression using the CRU TS data as the independent variable and the actual data as the dependent variable. The linear model created was used to correct the CRU TS data and create a time series for the period 1980–2020. This adjustment was made for the average annual temperature and the annual precipitation.

The effect of climate change on the xerothermality of the study area and the estimation of the xerothermality trends was also performed by analyzing a time series of Landsat TM and OLI satellite images for the period 1984–2022. A total of 107 images were analyzed (Table A1) with a sensed period from June to August. The year 2013 is not included in the analysis as there are no TM or OLI data available for that year, and ETM data are not used due to the error experienced by this sensor since May 2003. This collection of images was not easy to be made due to the relatively low temporal resolution and the lack of images for some months. As a result, an analysis on a monthly basis and for this time period would have many data gaps, even for some summer months. This is why we decided to restrict our analysis during the summer period alone. The spectral characteristics of Landsat TM and OLI images are presented in Table 1.

Table 1. Spectral and spatial characteristics of Landsat TM and OLI images.

Landsat 5-TM	Landsat 8-OLI
	B1—Coastal/Aerosol (0.435–0.451)—30 m
B1—Blue (0.45–0.52)—30 m	B2—Blue (0.452–0.512)—30 m
B2—Green (0.52–0.60)—30 m	B3—Green (0.533–0.590)—30 m
B3—Red (0.63–0.69)—30 m	B4—Red (0.636–0.673)—30 m
B4—NIR (0.76–0.90)—30 m	B5—NIR (0.851–0.879)—30 m
B5—SWIR 1 (1.55–1.75)—30 m	B6—SWIR 1 (1.566–1.651)—30 m
B7—SWIR 2 (2.08–2.35)—30 m	B7—SWIR 2 (2.107–2.294)—30 m
B6—TIR (10.40–12.50)—120 m	B10—TIR 1 (10.60–11.19)—30 m
	B11—TIR 2 (11.50–12.51)—30 m
	B9—Cirrus (1.363–1.384)—30 m
	B8—Pan (0.503–0.676)—15 m

The assessment of xerothermality trends was based on two indices, the Vegetation Condition Index (VCI) and the Temperature Condition Index (TCI) [39–41,43,51,52]. The TCI is based on the long-term assessment of the land surface temperature (LST), which is calculated from the single thermal channel of Landsat TM (Band 6) and from Band 10 of the two thermal channels of Landsat OLI (Bands 10 and 11). Then, the TCI index for each time slot is calculated by the following Formula (1):

$$TCIi = \frac{LSTmax - LSTi}{LSTmax - LSTmin} \quad (1)$$

where

TCIi = The TCI at the time i for a given pixel;

LSTmax = The maximum LST during the entire time series for a given pixel;

LSTmin = The minimum LST value the entire time series for a given pixel;

LSTi = The LST value at the time i for a given pixel.

TCI values range between 0 and 1, with values close to zero indicating strongly xerothermic conditions and values close to 1 indicating no xerothermic conditions.

Calculating surface temperature from satellite images is one of the most efficient ways for spatiotemporal monitoring of the thermal environment [53], while the methodology followed to estimate the LST from Landsat TM and OLI is one of the most reliable and widely used methods in the international literature. Much of the information we use to advance our equations is given by the MTL files of the images and is given in Table 2 below.

Table 2. Parameters for calculating LST from Landsat images.

Satellite-Sensor	K1	K2
Landsat TM	607.76	1260.56
Landsat OLI BAND 10	774.89	1321.08

Calculating LST from Landsat data, which have been already processed at Level 1C (geometrically corrected), involves the conversion of digital number values (DN) to top-of-atmosphere (ToA) radiance (L_λ) using the following Formula (2):

$$L_\lambda = M_\lambda * Q_{cal} + A_L \quad (2)$$

where

L_λ = Spectral radiance ($W/m^2 \cdot sr \cdot \mu m$);

M_λ = Radiance multi-band (found in the metadata file);

Qcal = The digital number value of the thermal band;

A_L = Radiance add band (found in the metadata file).

The next step is to convert Radiance values (A_λ) to Brightness Temperature (T_B) (in Kelvin) using the following Formula (3):

$$T_B = \frac{K2}{\ln\left(\frac{K1}{L\lambda} + 1\right)} \quad (3)$$

where

T_B = Brightness temperature in Kelvin;

K1 and K2 = Pre-launch calibration constants (shown in Table 2).

The land surface emissivity (ε) factor is critical for the calculation of LST because it adjusts the value of brightness temperature according to the land cover, and its calculation is based on the Normalized Difference Vegetation Index (NDVI).

NDVI is the most widely used vegetation index in remote sensing, and it is calculated using the near infrared and red bands according to Formulas (4) and (5):

$$NDVI(LandsatTM) = \frac{BAND4 - BAND3}{BAND4 + BAND3} \quad (4)$$

$$NDVI(Landsat\ OLI) = \frac{BAND5 - BAND4}{BAND5 + BAND4} \quad (5)$$

The emissivity was calculated using the following Formula (6):

$$\varepsilon = 0.004 * PV + 0.986 \quad (6)$$

PV stands for percentage vegetation and is calculated using the NDVI values and the following Formula (7):

$$PV = \left(\frac{NDVI - NDVI_{min}}{NDVI_{max} - NDVI_{min}}\right)^2 \quad (7)$$

where

NDVI = The NDVI value of a given pixel;

NDVImin = The minimum NDVI value across the study area;

NDVImax = The maximum NDVI value across the study area.

LST is calculated using the following Formula (8):

$$\mathrm{LST} = \mathrm{BT}/(1 + \mathrm{W} * (\mathrm{BT}/\mathrm{P}) * \ln(\varepsilon)) \quad (8)$$

where

LST = Land surface temperature in Kelvin;

BT = Brightness temperature;

W = The central band wavelength of emitted radiance (11.45 μm for Band 6 of Landsat TM and 10.9 μm for Band 10 of Landsat OLI);

P = 14,380 μmK;

ε = Land surface emissivity.

Finally, the calculated LST in Kelvin is converted to LST in degrees Celsius using the following Formula (9), and it was then applied to Formula (1) for calculating the TCI:

$$\mathrm{LSTcelcius} = \mathrm{LSTkelvin} - 273.15 \quad (9)$$

The Vegetation Condition Index is calculated using the following Formula (10), and it is based on the NDVI, which is calculated using Formulas (4) and (5) for Landsat TM and OLI, respectively.

$$VCIi = \frac{\mathrm{NDVIi} - \mathrm{NDVImin}}{\mathrm{NDVImax} - \mathrm{NDVImin}} \quad (10)$$

where

VCIi = The Vegetation Condition Index of a pixel at the time i;

NDVImax=The maximum NDVI during the entire time series for a given pixel;

NDVI min = The minimum NDVI during the entire time series for a given pixel;

NDVIi = The NDVI value of a pixel at the time i.

Both the TCI and VCI were calculated at an annual basis by averaging the corresponding values of the indices for each year, and they both serve as proxies for relevant climatic trends and vegetation condition. The first one, because it is based on the calculation of the surface temperature, can show the tendency to increase or decrease drought due to the increased or decreased, respectively, evapotranspiration as a result of higher temperature. The second one, because it is based on the NDVI, highlights the ecophysiological reaction of the vegetation to its inability to meet its water needs in order to carry out the physiological processes, primarily the process of photosynthesis [54]. According to the literature, the TCI and VCI values can be classified in drought-severity classes as shown in Table 3 [43].

Table 3. Classification of TCI and VCI into drought-severity classes.

Drought Class	TCI	VCI
Extremely severe	0–0.1	0–0.1
Severe	0.1–0.2	0.1–0.2
Moderate	0.2–0.3	0.2–0.3
Low	0.3–0.4	0.3–0.4
No drought	0.4–1	0.4–1

The trends in all studied meteorological parameters and generated indices were investigated using the Mann–Kendall test [55], which was performed using the XLSTAT extension of Microsoft Excel.

3. Results

3.1. Analysis of Climatic Data

As already mentioned, the climate data provided by the local weather station of the Meteo network (https://www.meteo.gr/index-en.cfm; accessed on 10 May 2023) were used to construct the Gausen and Bagnouls climatic diagram, which is shown in Figure 3.

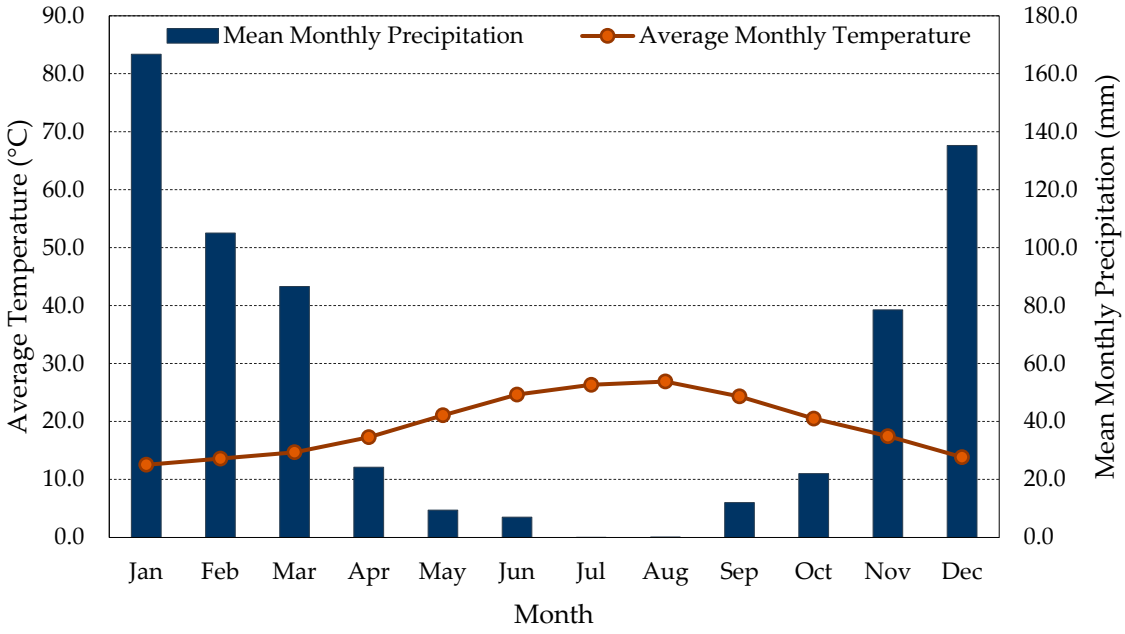


Figure 3. Gausen and Bagnouls climatic diagram for the period 2013–2021.

The climatic diagram highlights the climatic peculiarities of the study area. Perhaps the most distinctive feature is the huge variation in the distribution of rainfall throughout the year, ranging from 166 mm in January to zero mm in July. Almost all of the annual rainfall, which is about 647 mm on average, falls in the period between November and March. This, as well as the relatively small variation of the average monthly temperature during the year, leads to a particularly prolonged dry and warm period that lasts from April to October.

Figure 4 shows the variation and trend of mean annual temperature for the period 2013–2021 based on the local data. According to these data, although there appears to be a slight upwards trend in the mean annual temperature, the Mann–Kendall trend test indicates that this trend is not statistically significant (p = 0.602, S = 6, Var(S) = 92.0, Z = 0.521). Similar conclusions can be drawn for the dynamics of annual precipitation presented in Figure 5. Again there, although there seems to be a stronger upwards trend in annual precipitation, the Mann–Kendall trend test indicates that it is not statistically significant (p = 0.251, S = 12, Var(S) = 92.0, Z = 1.147). Therefore, in this case as well, no safe conclusions can be drawn about the dynamics of the annual rainfall from the data of the Fournoi MS.

In order to create a longer time series of data, the local climate data were used to fit a linear model between them and the CRU TS, thus creating a time series from 1980 to 2020. Figure 6 shows the results of the linear regression between the monthly temperature values given by the CRU TS data and the monthly temperature (MT) data collected from the local MS.

As shown in Figure 6, the prediction model of the actual monthly average temperature values from the CRU TS data is statistically significant, while the R^2 value, which is 0.9873, shows that there is an excellent fit between the observed data from the local MS and the CRU TS data. This is further confirmed in Figure 7, which shows the excellent fit between the observed data from the local MS and the corrected CRU TS data, which were corrected using the above model. Both findings justify that the adopted approach to generate a long time series dataset is accurate and that the generated time series of the average annual temperatures is expected to be very close to the real data.

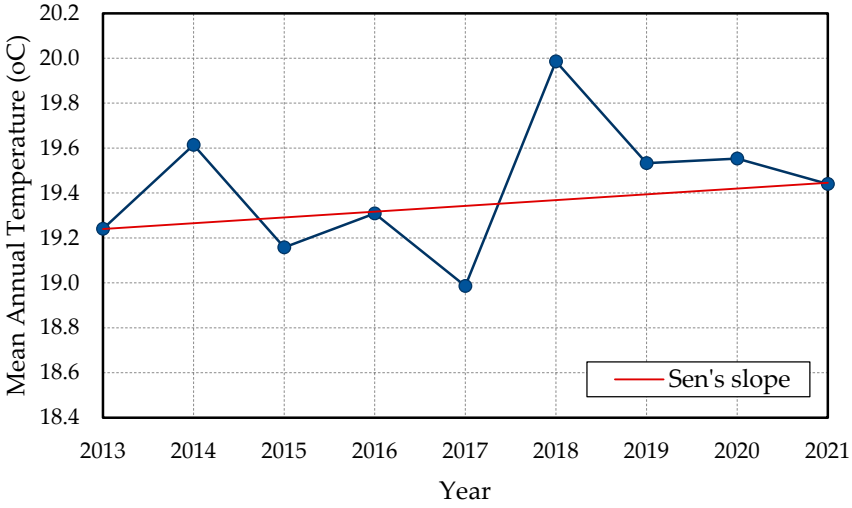


Figure 4. Mean annual temperature trend for the period 2013–2021 based on the actual local climatic data.

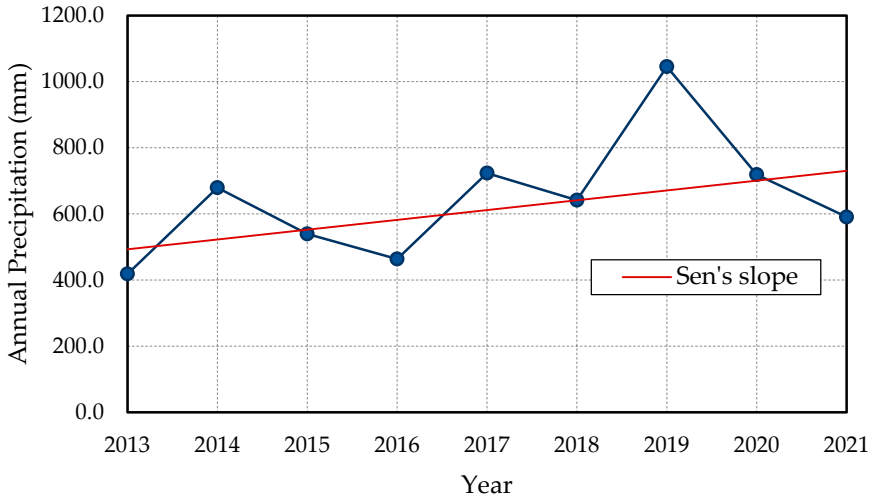


Figure 5. Annual precipitation trend for the period 2013–2021 based on the actual local climatic data.

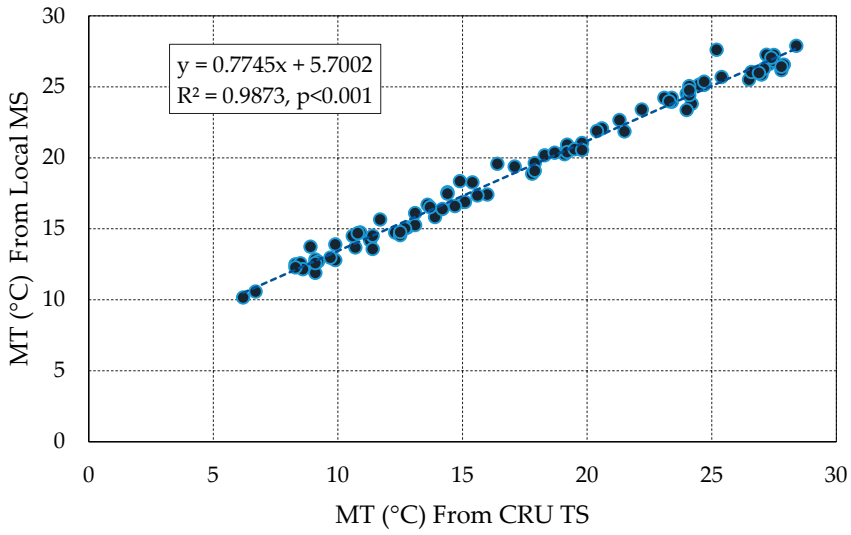


Figure 6. Linear regression model between the mean monthly temperature given by the CRU TS data and the actual local data.

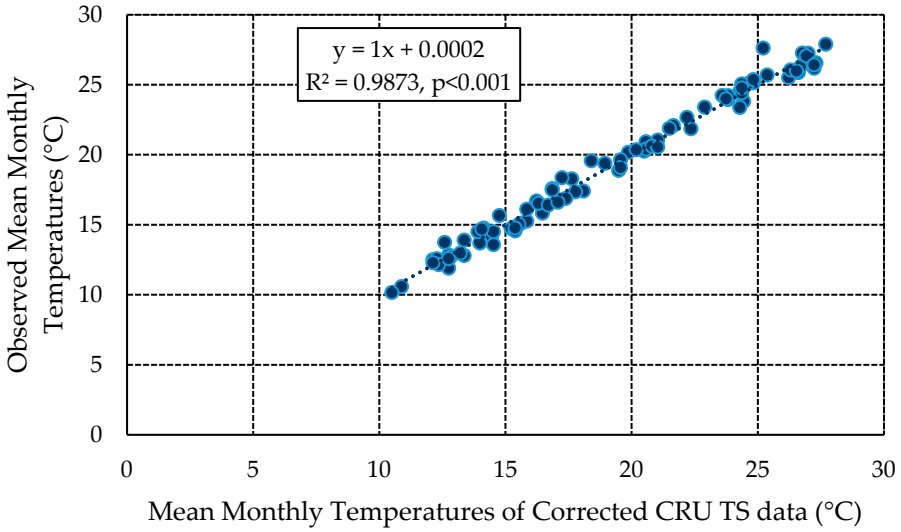


Figure 7. Observed data from the local MS vs. corrected CRU TS data based on the built model.

Using the corrected CRU TS data, a time series of mean annual temperature was generated for the period 1980–2020, and a trend analysis using Mann–Kendall trend test was performed (Figure 8). As clearly shown in Figure 8, there is a strong and statistically significant increasing trend of the mean annual temperature in the study area, which is confirmed by the results of the Mann–Kendall trend test ($p < 0.0001$, S = 463, Var(S) = 7925.667, Z = 5.189). This trend is expected to be confirmed in the analysis of xerothermic indicators obtained from the use of remote sensing data.

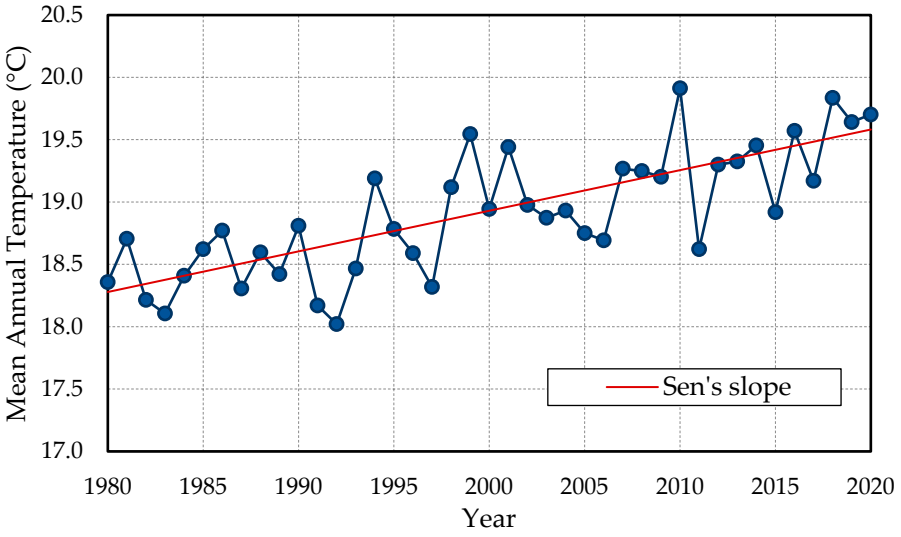


Figure 8. Trends of mean annual temperature across the period 1980–2020 based on the corrected CRU TS data.

The same approach was followed for the monthly precipitation (MP) data in order to obtain a long time series dataset of annual precipitation, although the results are not as accurate as those for the temperature data. The fitted linear regression model between the CRU TS values and local MS data, which is shown in Figure 9, shows that the model is statistically significant, but the value of R^2, which does not exceed 0.78, suggests that the interpretation of the corrected CRU TS data should be carried out with caution. The application of the linear regression model for the correction of the CRU TS data led to some negative values, which were adjusted to zero.

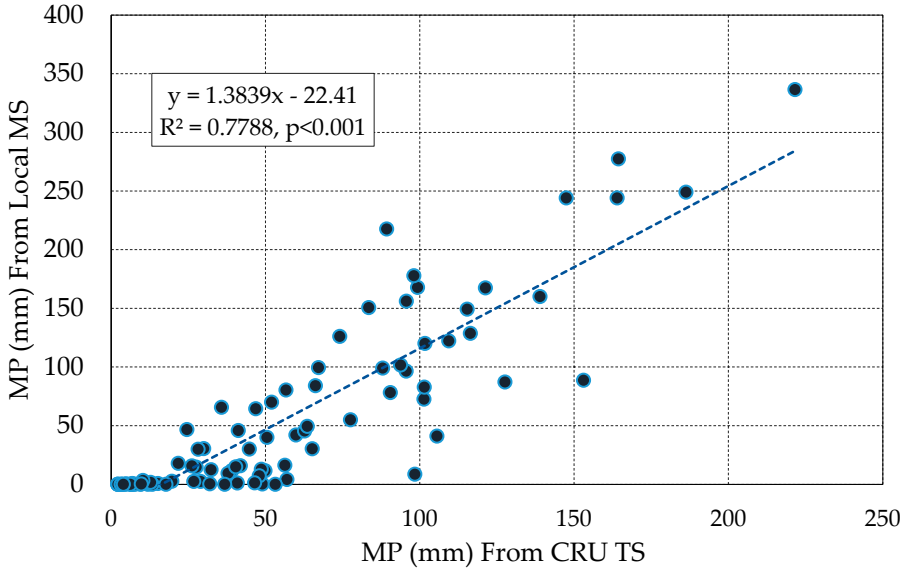


Figure 9. Linear regression model between the monthly precipitation given by the CRU TS data and the actual local data.

Unlike the temperature trend that was presented earlier, the temporal dynamics of the annual precipitation (Figure 10) and the performed Mann–Kendall trend test shows that although there is a slight increasing trend in annual precipitation, it is not statistically significant (p = 0.189, S = 118, Var(S) = 7926.667, Z = 1.314). It appears that there is an interannual variation, which is absolutely normal, that fluctuates around an average of 652 mm of precipitation per year. This average value is very close to the value of 647 mm of annual precipitation measured by the local MS for the period 2013–2021, and it is greater than the value of 623 mm obtained from the original CRU TS data. Although the annual precipitation shows a relative stability with a non-significant increasing trend, a separate analysis for the precipitation of October (Figure 11), which coincides with the end of the dry season, shows that, in October, there is a statically significant increasing trend in precipitation (p = 0.007, S = 241, Var(S) = 7882.333, Z = 2.703). However, it has to be noted that there is a high interannual variability in October's precipitation, which varies between zero precipitation and almost 180 mm.

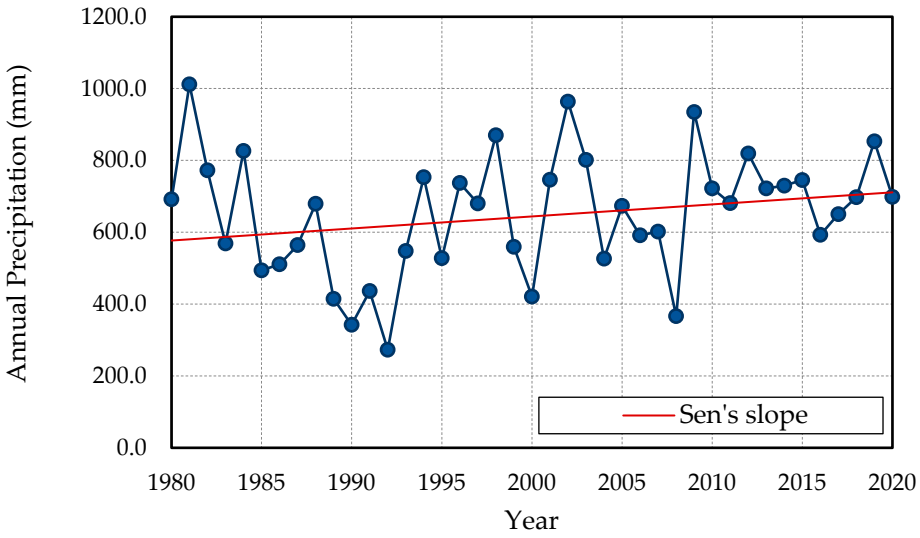


Figure 10. Trends of annual precipitation across the period 1980–2020 based on the corrected CRU TS data.

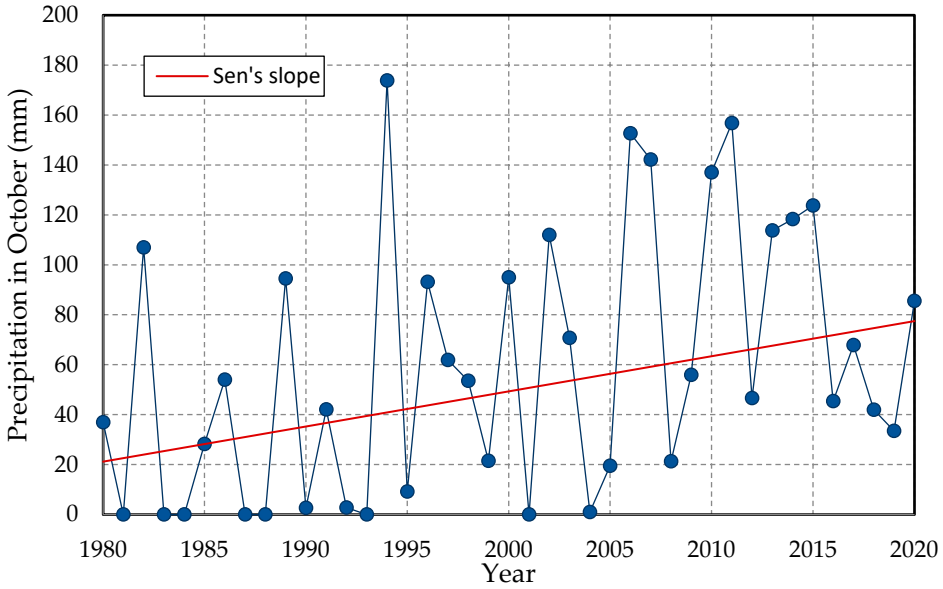


Figure 11. Trends of precipitation in October across the period 1980–2020 based on the corrected CRU TS data.

3.2. Analysis of Remote-Sensing-Derived Drought Indices

The analysis presented above shows a statistically significant increasing trend in air temperature over the last 40 years in the study area. At the same time, the analysis showed a stability in the amount of annual precipitation. Although the precipitation has an apparent interannual variation, it appears to be fluctuating around an annual mean of approximately 650 mm of rain. In order to examine the effect of these trends on the xerothermality of the area, a series of analyses was carried out using remote sensing data and the drought indices of the Temperature Condition Index (TCI) and Vegetation Condition Index (VCI), which are presented in the international literature and have been applied in practice with significant results. Figure 12 shows how the TCI evolved during the study period from 1984 until 2022. As one can see, apart from the obvious decrease in TCI (increase in xerothermality), there is a spatial variation across the island, which shows how the geomorphology can also affect xerothermality. Although it is beyond the scope of the study to investigate the effect of spatial heterogeneity on the xerothermality trend, it is an interesting area for future research.

The long-term trend analysis of the TCI, using the Mann–Kendall trend test (Figure 13), revealed that there is a dynamic and statistically significant trend of increasing drought, as estimated by surface temperature, during the period 1984–2022 ($p < 0.0001$, $S = -386$, $Var(S) = 6326$, $Z = -4.84057$). Until about the beginning of the 21st century, the variation in the index appears to be almost consistently above the non-drought threshold. On the contrary, after the year 2000, and especially in the last few years, it moves downwards, passing from the limits of moderate drought to those of intense and, in some cases, to the levels of extremely intense drought. This observation is in accordance with the observations made earlier based on the analysis of the climate data. It appears that an increase of about one degree Celsius in air temperature leads to an even more pronounced increase in drought, as estimated by the surface temperature. If this observation is combined with the distribution of rainfall and its restriction to only a short period during the year, it highlights the high sensitivity of the region to climate change. In ecological research and analysis, however, beyond the conditions that are formed, the impact they have on the ecophysiology of the vegetation is of particular importance.

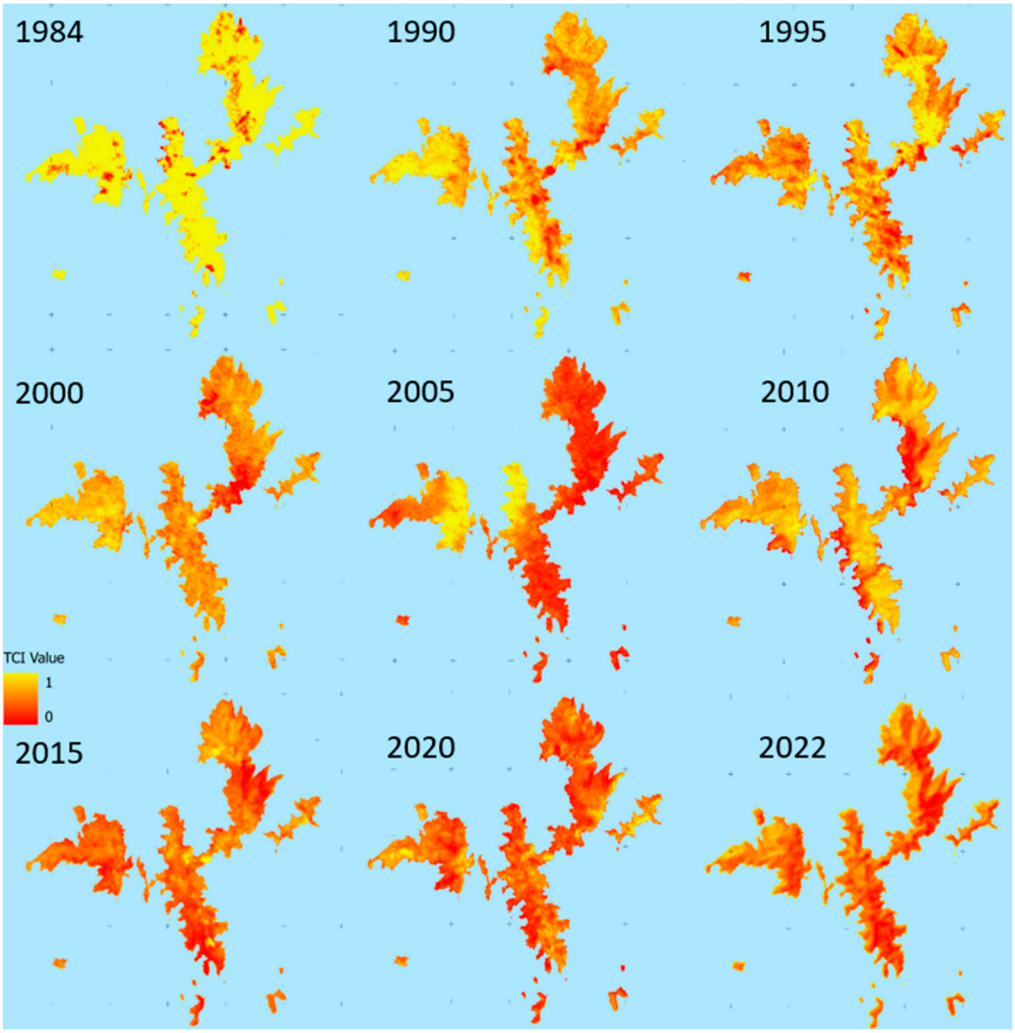


Figure 12. Evolution of the TCI across the study period using selected dates.

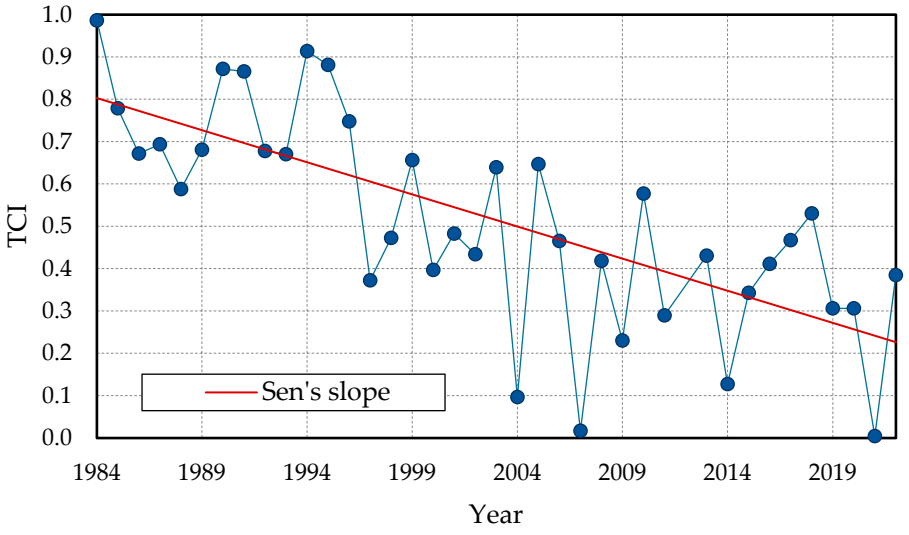


Figure 13. Trends of TCI for the period 1984–2022.

To analyze the effects of the increase in drought, due to the increase in temperature, on the vegetation of the study area, the VCI was employed. The logical assumption is that this increase in drought would result in a gradual increase of stress in the plants that compose

the main vegetation types of the area, during the summer months, for which this particular analysis is carried out. However, the results of the analysis of the long-term trends of the VCI (Figure 14) do not seem to verify this hypothesis.

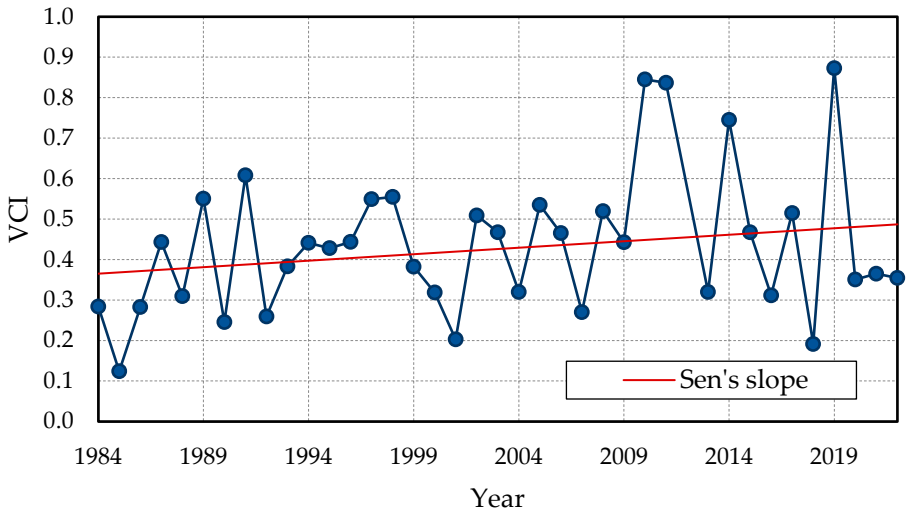


Figure 14. Trend of VCI for the period 1984–2022.

The VCI appears to remain stable throughout the time period, varying mainly between values of 0.2 and 0.6, with most years being between 0.2 and 0.5. This means that the vegetation of the area is facing some level of drought; however, it is not increasing since the Mann–Kendall trend tests do not show any statistically significant trend in VCI over the study period ($p < 0.152$, S = 115, Var(S) = 6327, Z = 1.433). At the same time, vegetation appears never to face extremely severe drought situations. It is rarely in severe drought situations, while it is usually at the levels of moderate or low drought and, in some cases, in the absence of drought. The fact that VCI has a much wider variation in the period after 2009 is also interesting.

4. Discussion

The results presented in the current study led to some safe conclusions in relation to the conditions of drought in this small island complex of the Eastern Aegean Sea. As the CRU TS meteorological data show, after their adjustment based on the actual data of the local MS, they indicate a statistically significant increasing trend of the average annual air temperature for the period 1980–2020 and a relative stability of the annual precipitation, however, with a significant interannual variation. The latter varies around a relatively high average of about 650 mm of precipitation per year. However, its dispersion throughout the year is limited to a very short period, leading to a dry period that lasts approximately for seven months. The analysis for precipitation trends in October alone, which signifies the beginning of autumn and the lowering of high temperatures, revealed an increasing trend, which was an interesting finding. There is clear evidence that land and sea surface temperature is increasing in the Mediterranean basin, and the latter is especially true in Eastern Mediterranean region [56]. At the same time, there is a growing amount of literature that demonstrates the significant role of sea surface temperature (SST) increase on precipitation patterns and precipitation extremes, especially around the Mediterranean region [57–61]. High SST may lead to increased evaporation and, as a result, increased concentration of moisture in the atmosphere. Increased concentration of moisture may also occur as a result of increased LST due to increased evapotranspiration (ET). After a hot and dry summer, in autumn the cooler air masses that descend from high atmospheric altitudes meet the warm and moist air masses near the surface causing atmospheric instability. This leads to the condensation of air moisture and subsequently to rainfall, which sometimes can be in the form of extreme rainfall events as the ones observed in 2024 in the eastern

Aegean. As the summers become hotter and drier and larger quantities of moisture are concentrated in the atmosphere it is reasonable to observe an increasing precipitation trend in the first months of Autumn. The increasing trend in October's precipitation is due to higher atmospheric instability from the seasonal transition of low-pressure systems from the central Mediterranean that is more pronounced because of the enhanced air-sea interaction caused by climate change. However, as it is recommended by Pastor et al. [62], further investigation is needed to directly associate increased SST and LST with precipitation patterns in Autumn since precipitation patterns depend on various other factors as well, such as circulation patterns and seasonal dynamics.

The results of the analysis of drought trends based on remote sensing data partly confirm the observation of increased drought throughout the study period since the TCI is significantly decreasing. However, the vegetation seems not to be negatively affected, which was an unexpected result. This interesting outcome not only does not diminish the value of the previous observation—that there is an increase in xerothermality in the region—but, on the contrary, makes its interpretation much more intriguing. This interpretation can only be understood in relation to the existing vegetation of the area. The vegetation composition and the ecosystems that prevail in the area, like almost all of the Aegean islands, have been formed through the influence of climatic, physiographic, and geological factors and, most importantly, through human activity over thousands of years [21,22]. In the study area, the dominant vegetation is the habitat type 5210, which is composed by species such as *R. lycioides*, *M. nervosa*, *A. ramosus,* and *M. comosum.* All of them, along with the dominant species *J. Phoenicea*, are thermophilic and xerophilic species [47]; as a result, they are adapted to dry conditions, which seem to allow them to withstand conditions of high xerothermality.

Another interpretation of the resistance of vegetation to increased drought severity lies in the vegetation and landscape dynamics of the area. After centuries of deforestation, land clearing, and overexploitation of forest resources, which have led to significant degradation of forests and shrublands, there has been a growing trend to reduce their exploitation for energy wood and other products over the last few decades. Furthermore, increasing agricultural land abandonment has been observed in several regions of Europe and the Mediterranean, both in insular and continental environments [14,16,18–21,46,63–66]. This change marks the beginning of the recovery process for many Mediterranean scrub ecosystems including the areas dominated by formations of *J. Phoenicea,* which most likely constitute the CLIMAX plant community of the region [21]. Therefore, the observed resistance of the vegetation and, more specifically, of type 5210 to the increasing drought conditions is a result of both the high drought resistance, due to its species composition, and the fact the vegetation is recovering after years of degradation and overexploitation.

The second-most abundant habitat type in the area is "*S. spinosum* phryganas—5420", characterized by the dominance of *S. spinosum* and the presence of species including *G. acanthoclada*, *T. capitatus*, *A. hermania*, *Cistus spp*, *E. verticilata,* etc. The formations of *S. spinosum* are also characterized for their drought resistance, while, according to Tzanopoulos et al. [21], they are characteristic formations of lands that have been degraded by the long-term pressures of grazing, wood extraction, and wildfires. These communities represent a degradation stage of communities dominated by *J. phoenicea*. Therefore, in this case too, it is the resistance of the vegetation to drought that leads to the absence of drought conditions, as assessed using the VCI.

Another interesting finding of this study is the fact that, in recent decades, there has been a much stronger interannual variation, both in VCI and TCI, indicating the interchange of years of extreme xerothermality and wet years. It is characteristic that 2007 is one of the years that TCI scores zero, indicating conditions of extreme xerothermality. This year was characterized by three consecutive heatwaves, starting from June and ending in August [67,68], which led to extremely dry conditions and the worst fire season ever in Greece with 200,000 ha of burned area. Founda and Gianakopoulos [67], Tolika et al. [68], and Nastos and Kapsomenakis [69] suggest that the extreme events of high air temperatures

are going to become more frequent in the 21st century, and, as a result, an intensified variability in climatic patterns is expected.

The socioeconomic impacts of increasing drought trends in the region are profound. Prolonged dry periods and rising temperatures significantly strain water resources, directly affecting agricultural productivity. This region relies heavily on agriculture, and reduced yields due to water scarcity can lead to substantial economic losses, food insecurity, and increased dependence on costly imported goods [70]. Moreover, the degradation of natural habitats as a result of intensified drought can negatively impact biodiversity, which in turn affects ecotourism—a vital sector for the local economy [71]. The resilience of drought-resistant vegetation, such as *J. phoenicea* and *S. spinosum*, while mitigating some ecological impacts, does not fully address the economic pressures faced by local communities. Adaptation strategies are crucial to manage these socioeconomic challenges effectively [72]. New environmental management approaches and strategies must take into consideration the optimal use of water resources, conservation activities, and agricultural activities. For the study area, which is agriculturally intensive in some parts, strategies such as rainwater harvesting, enhanced irrigation methods, and the use of drought-tolerant crops could help the islands to address challenges related to water shortage [73]. However, the sources of these strategies are from interests that are not always easy to get from diverse actors such as farmers, conservationists, or local authorities.

Policymakers could draw experience from successful case studies in other Mediterranean areas, for example, the sustainable water management policies adopted in Cyprus [74]. Furthermore, the creation of multi-stakeholder policy communities would provide a forum for addressing different views on adequate distribution of resources. Such planning processes can be appropriate since local people would be empowered to adopt sustainable solutions that would address the specific needs of the area. The Fournoi complex can come up with effective, fair, and holistic adaptation strategies by adapting in the local conditions several experiences from similar regions and enhancing collaboration among the stakeholders.

In this study, we used two types of data to investigate the trends of aridity and drought in a small insular environment. The first set of data used temperature and precipitation that have been adjusted based on linear models between interpolated values and actual local measurements. Despite the high coefficients of determination that were achieved in these models, one should always bear in mind that they are not actual measurements from local meteorological stations, and this constitutes a limitation of the study. However, the approach adopted and presented here allows the creation of a long time series of the two basic climatic parameters, of precipitation and temperature, using local data of a short period of time or data that are interrupted. The availability of long-term meteorological data is extremely low in many places across the globe and the presented method provides a valuable alternative. The study also used remote sensing derived indices (VCI and TCI) to investigate long-term trends of xerothermality. Both indices have of course some limitations. They are mainly based on single-dimensional information of vegetation and temperature and may not fully reflect the comprehensive characteristics of drought, including soil moisture deficit and atmospheric water balance. In addition, the determination of index thresholds may be subjective and regional, which may affect the accurate assessment of drought severity. Another limitation of the study is the fact that we did not investigate the role of spatial heterogeneity on the observed xerothermality. This investigation will provide useful insights on the conservation status of many ecologically significant habitats in this and in other similar environments. Finally, the value of this research is concentrated on the determination of long-term trends in xerothermality and vegetation condition but does not incorporate the influence of the precipitation-to-evapotranspiration (P/ETa) patterns, which are decisive factors for the development, duration, and severity of drought events effecting the ecosystems. P/ETa, also called the Aridity Index (AI), is increasingly important as indicators of water balance within an ecosystem. The fact that the above study has no information about changes in P has occurred because the availability of accurate ETa data

requires high-resolution modeling or field-based measurements, which were not available in the current study. Future studies should have a P/ETa integration component, including modeled ETa datasets or local monitoring systems, to understand better the impact of droughts on vegetation water dynamics.

5. Conclusions

This study highlights significant climatic trends and their implications for drought conditions on a small island in the Eastern Aegean Sea. The analysis of adjusted CRU TS meteorological data, supported by local measurements, shows a significant increase in average annual air temperature over the past four decades, alongside stable but variably distributed annual precipitation. This has resulted in a prolonged dry period of about seven months each year, increasing xerothermality in the region. The remote sensing analysis confirms a significant upward trend in drought severity through a decreasing Temperature Condition Index (TCI). However, the Vegetation Condition Index (VCI) did not show increased vegetation stress, indicating the resilience of local flora, and species like *J. phoenicea* and *S. spinosum*. This resilience is attributed in the current study to the drought-resistant nature of these species and ongoing ecological recovery following historical land use. However, other factors may have a significant contribution on the resistance of vegetation to increasing xerothermality, including soil chemical and physical properties, geomorphology, land use history of various parts of the island, disturbance history, and others. This constitutes an important area for future research, and this research team is already working towards this direction. Despite ecological resilience, the increasing drought poses socioeconomic challenges. Agricultural productivity is likely to decline, leading to economic losses and food security concerns. Additionally, habitat degradation may impact biodiversity and ecotourism, vital for the local economy. Therefore, urgent attention and adaptive management strategies are needed to address these challenges.

In conclusion, while the vegetation shows resilience, the broader socioeconomic implications of increasing drought require comprehensive management strategies that integrate scientific insights with practical solutions to ensure sustainable development in the Eastern Aegean islands. Future research should refine these strategies to mitigate the adverse effects of drought in this sensitive region.

Author Contributions: Conceptualization, P.X. and D.E.; methodology, P.X., S.C., G.K. and P.N.; software, P.X., G.K. and S.C.; validation, P.X., D.E. and P.N.; formal analysis, P.X., G.K. and S.C.; investigation, P.X., E.F., E.S., K.K., G.K. and S.C.; resources, D.E.; data curation, P.X. and P.N.; writing—original draft preparation, P.X. and E.F.; writing—review and editing, P.X., P.N. and E.F.; visualization, P.X. and E.F.; supervision, D.E.; project administration, K.K.; funding acquisition, D.E. All authors have read and agreed to the published version of the manuscript.

Funding: This research was part of the research project entitled: "Addressing water resource scarcity of small arid islands"—Coordinator: International Hellenic University. The project was funded by the Secretary General of the Aegean and Island Policy, Ministry of Maritime Affairs and Insular Policy, Greece. Contract Number 559/2022.

Data Availability Statement: The data that support the findings of this study are available on request from the corresponding author, P.X.

Conflicts of Interest: The authors declare no conflicts of interest.

Appendix A

Table A1. Landsat TM and OLI images that were used in the analysis.

Image Name	Acquisition Date
LT05_L1TP_181034_19840619_20200918_02_T1	19/06/1984
LT05_L1TP_181034_19840721_20200918_02_T1	21/07/1984
LT05_L1TP_181034_19840806_20200918_02_T1	06/08/1984

Table A1. *Cont.*

Image Name	Acquisition Date
LT05_L1TP_181034_19850708_20200918_02_T1	08/07/1985
LT05_L1TP_181034_19850809_20200918_02_T1	09/08/1985
LT05_L1TP_181034_19860609_20200917_02_T1	09/06/1986
LT05_L1TP_181034_19860727_20200918_02_T1	27/07/1986
LT05_L1TP_181034_19860812_20200918_02_T1	12/08/1986
LT05_L1TP_181034_19870612_20201014_02_T1	12/06/1987
LT05_L1TP_181034_19870714_20201014_02_T1	14/07/1987
LT05_L1TP_181034_19870831_20201014_02_T1	31/08/1987
LT05_L1TP_181034_19880630_20200917_02_T1	30/06/1988
LT05_L1TP_181034_19880716_20200917_02_T1	16/07/1988
LT05_L1TP_181034_19880801_20200917_02_T1	01/08/1988
LT05_L1TP_181034_19890516_20200916_02_T1	16/05/1989
LT05_L1TP_181034_19890719_20200916_02_T1	19/07/1989
LT05_L1TP_181034_19890820_20200916_02_T1	20/08/1989
LT05_L1TP_181034_19900620_20200916_02_T1	20/06/1990
LT05_L1TP_181034_19900722_20200916_02_T1	22/07/1990
LT05_L1TP_181034_19900807_20200915_02_T1	07/08/1990
LT05_L1TP_181034_19910623_20200915_02_T1	23/06/1991
LT05_L1TP_181034_19910709_20200915_02_T1	09/07/1991
LT05_L1TP_181034_19910810_20200915_02_T1	10/08/1991
LT05_L1TP_181034_19920609_20200914_02_T1	09/06/1992
LT05_L1TP_181034_19920711_20200914_02_T1	11/07/1992
LT05_L1TP_181034_19920828_20200914_02_T1	28/08/1992
LT05_L1TP_181034_19930815_20200913_02_T1	15/08/1993
LT05_L1TP_181034_19930730_20200913_02_T1	30/07/1993
LT05_L1TP_181034_19930628_20200914_02_T1	28/06/1993
LT05_L1TP_181034_19940530_20200913_02_T1	30/05/1994
LT05_L1TP_181034_19940802_20200913_02_T1	02/08/1994
LT05_L1TP_181034_19950618_20211122_02_T1	18/06/1995
LT05_L1TP_181034_19950720_20200912_02_T1	20/07/1995
LT05_L1TP_181034_19950821_20200912_02_T1	21/08/1995
LT05_L1TP_181034_19960604_20200911_02_T1	04/06/1996
LT05_L1TP_181034_19960706_20200911_02_T1	06/07/1996
LT05_L1TP_181034_19960807_20200911_02_T1	07/08/1996
LT05_L1TP_181034_19970623_20200910_02_T1	23/06/1997
LT05_L1TP_181034_19970709_20200910_02_T1	09/07/1997
LT05_L1TP_181034_19970810_20200910_02_T1	10/08/1997
LT05_L1TP_181034_19980610_20200909_02_T1	10/06/1998
LT05_L1TP_181034_19980728_20200908_02_T1	28/07/1998
LT05_L1TP_181034_19980829_20200908_02_T1	29/08/1998
LT05_L1TP_181034_19990613_20200908_02_T1	13/06/1999
LT05_L1TP_181034_19990731_20200908_02_T1	31/07/1999
LT05_L1TP_181034_19990816_20200908_02_T1	16/08/1999
LT05_L1TP_181034_20000615_20200907_02_T1	15/06/2000
LT05_L1TP_181034_20000717_20200906_02_T1	17/07/2000
LT05_L1TP_181034_20000818_20200906_02_T1	18/08/2000
LT05_L1TP_181034_20010618_20200906_02_T1	18/06/2001
LT05_L1TP_181034_20010720_20200905_02_T1	20/07/2001
LT05_L1TP_181034_20010821_20200905_02_T1	21/08/2001
LT05_L1TP_181034_20020605_20200905_02_T1	05/06/2002
LT05_L1TP_181034_20020723_20200905_02_T1	23/07/2002
LT05_L1TP_181034_20030624_20200904_02_T1	24/06/2003
LT05_L1TP_181034_20030726_20200904_02_T1	26/07/2003
LT05_L1TP_181034_20030811_20200904_02_T1	11/08/2003
LT05_L1TP_181034_20040626_20200903_02_T1	26/06/2004
LT05_L1TP_181034_20040712_20200903_02_T1	12/07/2004
LT05_L1TP_181034_20040813_20200903_02_T1	13/08/2004
LT05_L1TP_181034_20050613_20200902_02_T1	13/06/2005
LT05_L1TP_181034_20050629_20200902_02_T1	29/06/2005

Table A1. *Cont.*

Image Name	Acquisition Date
LT05_L1TP_181034_20050816_20200902_02_T1	16/08/2005
LT05_L1TP_181034_20060616_20200901_02_T1	16/06/2006
LT05_L1TP_181034_20060718_20200831_02_T1	18/07/2006
LT05_L1TP_181034_20060819_20200831_02_T1	19/08/2006
LT05_L1TP_181034_20070721_20211210_02_T1	21/07/2007
LT05_L1TP_181034_20070822_20200830_02_T1	22/08/2007
LT05_L1TP_181034_20080621_20200829_02_T1	21/06/2008
LT05_L1TP_181034_20080707_20200829_02_T1	07/07/2008
LT05_L1TP_181034_20080808_20200829_02_T1	08/08/2008
LT05_L1TP_181034_20090608_20200827_02_T1	08/06/2009
LT05_L1TP_181034_20090726_20200827_02_T1	26/07/2009
LT05_L1TP_181034_20090827_20200825_02_T1	27/08/2009
LT05_L1TP_181034_20100526_20200824_02_T1	26/05/2010
LT05_L1TP_181034_20100713_20200823_02_T1	13/07/2010
LT05_L1TP_181034_20110630_20200822_02_T1	30/06/2011
LT05_L1TP_181034_20110716_20200822_02_T1	16/07/2011
LT05_L1TP_181034_20110801_20200820_02_T1	01/08/2011
LC08_L1TP_181034_20130619_20200912_02_T1	19/06/2013
LC08_L1TP_181034_20130721_20200912_02_T1	21/07/2013
LC08_L1TP_181034_20130822_20200913_02_T1	22/08/2013
LC08_L1TP_181034_20140622_20200911_02_T1	22/06/2014
LC08_L1TP_181034_20140708_20200911_02_T1	08/07/2014
LC08_L1TP_181034_20140825_20200911_02_T1	25/08/2014
LC08_L1TP_181034_20150625_20200909_02_T1	25/06/2015
LC08_L1TP_181034_20150727_20200908_02_T1	27/07/2015
LC08_L1TP_181034_20150828_20200908_02_T1	28/08/2015
LC08_L1TP_181034_20160611_20200906_02_T1	11/06/2016
LC08_L1TP_181034_20160729_20200906_02_T1	29/07/2016
LC08_L1TP_181034_20160830_20200906_02_T1	30/08/2016
LC08_L1TP_181034_20170614_20200903_02_T1	14/06/2017
LC08_L1TP_181034_20170716_20200903_02_T1	16/07/2017
LC08_L1TP_181034_20170817_20200903_02_T1	17/08/2017
LC08_L1TP_181034_20180719_20200831_02_T1	19/07/2018
LC08_L1TP_181034_20180820_20200831_02_T1	20/08/2018
LC08_L1TP_181034_20190620_20200827_02_T1	20/06/2019
LC08_L1TP_181034_20190722_20200827_02_T1	22/07/2019
LC08_L1TP_181034_20190823_20200826_02_T1	23/08/2019
LC08_L1TP_181034_20200521_20200820_02_T1	21/05/2020
LC08_L1TP_181034_20200708_20200912_02_T1	08/07/2020
LC08_L1TP_181034_20200825_20200905_02_T1	25/08/2020
LC08_L1TP_181034_20210625_20210707_02_T1	25/06/2021
LC08_L1TP_181034_20210727_20210804_02_T1	27/07/2021
LC08_L1TP_181034_20210828_20210901_02_T1	28/08/2021
LC08_L1TP_181034_20220730_20220806_02_T1	30/07/2022
LC09_L1TP_181034_20220807_20230403_02_T1	07/08/2022

References

1. Suc, J.P. Origin and evolution of the Mediterranean vegetation and climate in Europe. *Nature* **1984**, *307*, 429–432. [CrossRef]
2. Blondel, J. The 'Design' of Mediterranean Landscapes: A Millennial Story of Humans and Ecological Systems during the Historic Period. *Hum. Ecol.* **2006**, *34*, 713–729. [CrossRef]
3. Blondel, J.; Aronson, J. Biodiversity and Ecosystem function in the Mediteranean Basin: Human and Non-Human Determinants. In *Mediterranean-Type Ecosystems. The function of Biodiversity*; Davis, G.W., Richardson, D.M., Eds.; Springer-Verlag: Berlin/Heidelberg, Germany, 1995; Volume 109, pp. 43–119.
4. Blondel, J.; Aronson, J.; Bodiou, J.Y.; Boeuf, G. The Mediterranean Region. In *Biological Diversity in Space and Time*, 2nd ed.; Oxford University Press: New York, NY, USA, 2010; p. 401.
5. Medail, F. The specific vulnerability of plant biodiversity and vegetation on Mediterranean islands in the face of global change. *Reg. Environ. Change* **2017**, *17*, 1775–1790. [CrossRef]
6. Medail, F. Plant Biogeography and Vegetation Patterns of the Mediterranean Islands. *Bot. Rev.* **2022**, *88*, 63–129. [CrossRef]

7. Myers, N.; Mittermeier, R.A.; Mittermeier, C.G.; da Fonseca, G.A.B.; Kent, J. Biodiversity hotspots for conservation priorities. *Nature* **2000**, *403*, 853–858. [CrossRef]
8. Cowling, R.M.; Rundel, P.W.; Lamnont, B.B.; Arroyo, M.; Arianoutsou, M. Plant diversity in mediterranean-climate regions. *Trends Ecol. Evol.* **1996**, *11*, 362–366. [CrossRef] [PubMed]
9. Gomez-Campo, C. The conservation of Mediterranean plants: Principles and problems. In *Plant Conservation in the Mediterranean area, Gomez-Campo, C., Ed.*; Dr W. Junk Publisher: Dordrecht, The Netherlands; Boston, MA, USA; Lancaster, UK, 1985; Volume 7, pp. 3–8.
10. Quezel, P. Definition of the Mediterranean region and the origin of its flora. In *Plant conservation in the Mediterranean Area, Gomez-Campo, C., Ed.*; Dr W. Junk Publishers: Dordrecht, The Netherlands; Boston, MA, USA; Lancaster, UK, 1985; Volume 7, pp. 9–24.
11. Scarascia-Mugnozza, G.; Oswald, H.; Piussi, P.; Radoglou, K. Forests of the Mediterranean region: Gaps in knowledge and research needs. *For. Ecol. Manag.* **2000**, *132*, 97–109. [CrossRef]
12. Cuttelod, A.; García, N.; Abdul Malak, D.; Temple, H.; Katariya, V. The Mediterranean: A biodiversity hotspot under threat. In *The 2008 Review of The IUCN Red List of Threatened Species, Vié, J.-C., Hilton-Taylor, C., Stuart, S.N., Eds.*; IUCN: Gland, Switzerland, 2008.
13. Kontsiotis, V.J.; Bakaloudis, D.E.; Xofis, P.; Konstantaras, N.; Petrakis, N.; Tsiompanoudis, A. Modeling the distribution of wild rabbits (Oryctolagus cuniculus) on a Mediterranean island. *Ecol. Res.* **2013**, *25*, 317–325. [CrossRef]
14. Vogiatzakis, I.N.; Mannion, A.M.; Griffiths, G.H. Mediterranean ecosystems: Problems and tools for conservation. *Prog. Phys. Geogr.* **2006**, *30*, 175–200. [CrossRef]
15. Medail, F.; Quezél, P. Biodiversity Hotspots in the Mediterranean Basin: Setting Global Conservation Priorities. *Conserv. Biol.* **1999**, *13*, 1510–1513. [CrossRef]
16. Tzanopoulos, J.; Vogiatzakis, I.N. Processes and patterns of landscape change on a small Aegean island: The case of Sifnos, Greece. *Landsc. Urban Plan.* **2011**, *99*, 58–64. [CrossRef]
17. Blondel, J. On humans and wildlife in Mediterranean islands. *J. Biogeogr.* **2008**, *35*, 509–518. [CrossRef]
18. Kefalas, G.; Kalogirou, S.; Poirazidis, K.; Lorilla, R.S. Landscape transition in Mediterranean islands: The case of Ionian islands, Greece 1985–2015. *Landsc. Urban Plan.* **2019**, *191*, 103641. [CrossRef]
19. Kefalas, G.; Poirazidis, K.; Xofis, P.; Kalogirou, S. Mapping and Understanding the Dynamics of Landscape Changes on Heterogeneous Mediterranean Islands with the Use of OBIA: The Case of Ionian Region, Greece. *Sustainbility* **2018**, *10*, 2986. [CrossRef]
20. Kefalas, G.; Poirazidis, K.; Xofis, P.; Kalogirou, S.; Chalkias, C. Landscape dynamics on insular environments of South-east mediterranean Europe. *Geocardo Int.* **2020**, *37*, 1–19. [CrossRef]
21. Tzanopoulos, J.; Mitchley, J.; Pantis, J.D. Modelling the Effects of Human Activity on the Vegetation of a Northeast Mediterranean Island. *Appl. Veg. Sci.* **2003**, *8*, 182–190. [CrossRef]
22. Petanidou, T.; Kizos, T.; Soulakelis, N. Socioeconomic Dimensions of Changes in the Agricultural Landscape of the Mediterranean Basin: A Case Study of the Abandonment of Cultivation Terraces on Nisyros Island, Greece. *Environ. Manag.* **2008**, *41*, 250–266. [CrossRef]
23. Mycoo, M.; Wairiu, M.; Campbell, D.; Duvat, V.; Golbuu, Y.; Maharaj, S.; Nalau, J.; Nunn, P.; Pinnegar, J.; Warrick, O. Small Islands. In *Climate Change 2022: Impacts, Adaptation and Vulnerability. Contribution of Working Group II to the Sixth Assessment Report of the Intergovernmental Panel on Climate Change*; Pörtner, H.-O., Roberts, D.C., Tignor, M., Poloczanska, E.S., Mintenbeck, K., Alegría, A., Craig, M., Langsdorf, S., Löschke, S., Möller, V., et al., Eds.; Cambridge University Press: Cambridge, UK; New York, NY, USA, 2022; pp. 2043–2121.
24. Pörtner, H.-O.; Roberts, D.C.; Adams, H.; Adelekan, I.; Adler, C.; Adrian, R.; Aldunce, P.; Ali, E.; Ara Begum, R.; Bednar-Friedl, B.; et al. 2022: Technical Summary. In *Climate Change 2022: Impacts, Adaptation and Vulnerability. Contribution of Working Group II to the Sixth Assessment Report of the Intergovernmental Panel on Climate Change*; Pörtner, H.-O., Roberts, D.C., Tignor, M., Poloczanska, E.S., Mintenbeck, K., Alegría, A., Craig, M., Langsdorf, S., Löschke, S., Möller, V., et al., Eds.; Cambridge University Press: Cambridge, UK; New York, NY, USA, 2022; pp. 37–118.
25. Ameca, E.I.; Nie, Y.; Wu, R.; Mittermeier, R.A.; Foden, W.; Wei, F. Identifying protected areas in biodiversity hotspots at risk from climate and human-induced compound events for conserving threatened species. *Sci. Total Environ.* **2024**, *938*, 173192. [CrossRef]
26. Habibullah, M.S.; Din, B.H.; Tan, S.-H.; Zahid, H. Impact of climate change on biodiversity loss: Global evidence. *Environ. Sci. Pollut. Res.* **2021**, *29*, 1073–1086. [CrossRef]
27. Malcolm, J.R.; Liu, C.; Neilson, R.P.; Hansen, L.; Hannah, L. Global Warming and Extinctions of Endemic Species from Biodiversity Hotspots. *Conserv. Biol.* **2006**, *20*, 538–548. [CrossRef]
28. Urban, M.C. Accelerating extinction risk from climate change. *Science* **2015**, *348*, 571–573. [CrossRef] [PubMed]
29. Galassi, G.; Spada, G. Sea-level rise in the Mediterranean Sea by 2050: Roles of terrestrial ice melt, steric effects and glacial isostatic adjustment. *Glob. Planettary Change* **2014**, *123*, 55–66. [CrossRef]
30. Giorfi, F.; Lionello, P. Climate change projections for the Mediterranean region. *Glob. Planettary Change* **2008**, *63*, 90–104. [CrossRef]
31. Lionello, P.; Abrantes, F.; Gacic, M.; Planton, S.; Trigo, R.; Ulbrich, U. The climate of the Mediterranean region: Research progress and climate change impacts. *Reg. Environ. Change* **2014**, *14*, 1679–1684. [CrossRef]
32. Mariotti, A.; Pan, Y.; Zeng, N.; Alessandri, A. Long-term climate change in the Mediterranean region in the context of global warming. *Clim. Dyn.* **2015**, *44*, 1437–1456. [CrossRef]

33. Zittis, G.; Hadjinicolaou, P.; Lelieveld, J. Role of soil moisture in the amplification of climate warming in the eastern Mediterranean and the Middle East. *Clim. Res.* **2014**, *59*, 27–37. [CrossRef]
34. Guiot, J.; Cramer, W. Climate change: The 2015 Paris Agreement thresholds and Mediterranean basin ecosystems. *Science* **2016**, *354*, 465–468. [CrossRef] [PubMed]
35. Beygi Heidarlou, H.; Gholamzadeh Bazarbash, M.; Borz, S.A. Unveiling the Role of Climate and Environmental Dynamics in Shaping Forest Fire Patterns in Northern Zagros, Iran. *Land* **2024**, *13*, 1453. [CrossRef]
36. Nath, N.; Sahariah, D.; Meraj, G.; Debnath, J.; Kumar, P.; Lahon, D.; Chand, K.; Farooq, M.; Chandan, P.; Singh, S.K.; et al. Land Use and Land Cover Change Monitoring and Prediction of a UNESCO World Heritage Site: Kaziranga Eco-Sensitive Zone Using Cellular Automata-Markov Model. *Land* **2022**, *12*, 151. [CrossRef]
37. Zhang, J.; Liu, X.; Qin, Y.; Fan, Y.; Cheng, S. Wetlands Mapping and Monitoring with Long-Term Time Series Satellite Data Based on Google Earth Engine, Random Forest, and Feature Optimization: A Case Study in Gansu Province, China. *Land* **2024**, *13*, 1527. [CrossRef]
38. Hussain, S.; Lu, L.; Mubeen, M.; Nasim, W.; Karuppannan, S.; Fahad, S.; Tariq, A.; Mousa, B.G.; Mumtaz, F.; Aslam, M. Spatiotemporal Variation in Land Use Land Cover in the Response to Local Climate Change Using Multispectral Remote Sensing Data. *Land* **2022**, *11*, 595. [CrossRef]
39. Kogan, F.N. Application of vegetation index and brightness temperature for drought detection. *Adv. Space Res.* **1995**, *15*, 91–100. [CrossRef]
40. Kogan, F.N. Droughts of the late 1980s in the United States as derived from NOAA polar-orbiting satellite data. *Bull. Am. Meteorol. Soc.* **1995**, *76*, 655–668. [CrossRef]
41. Kogan, F.N. Global drought watch from space. *Bull. Am. Meteorol. Soc.* **1997**, *78*, 621–636. [CrossRef]
42. Urban, M.; Berger, C.; Mudau, T.E.; Heckel, K.; Truckenbrodt, J.; Onyango Odipo, V.; Smit, I.P.J.; Schmullius, C. Surface Moisture and Vegetation Cover Analysis for Drought Monitoring in the Southern Kruger National Park Using Sentinel-1, Sentinel-2, and Landsat-8. *Remote Sens.* **2018**, *10*, 1482. [CrossRef]
43. Wei, W.; Zhang, J.; Zhou, L.; Xie, B.; Zhou, J.; Li, Q. Comparative evaluation of drought indices for monitoring drought based on remote sensing data. *Environ. Sci. Pollut. Res.* **2021**, *28*, 20408–20425. [CrossRef] [PubMed]
44. Peters, A.J.; Walter-Shea, E.A.; Ji, L.; Vina, A.; Hayes, M.; Svoboda, M.D. Drought monitoring with NDVI-based standardized vegetation index. *Photogramm. Eng. Remote Sens.* **2002**, *68*, 71–75.
45. Xofis, P.; Buckley, G.P.; Takos, I.; Mitchley, J. Long Term Post-Fire Vegetation Dynamics in North-East Mediterranean Ecosystems. The Case of Mount Athos Greece. *Fire* **2021**, *4*, 92. [CrossRef]
46. Xofis, P.; Spiliotis, J.A.; Chatzigiovanakis, S.; Chrysomalidou, A.S. Long-Term Monitoring of Vegetation Dynamics in the Rhodopi Mountain Range National Park-Greece. *Forests* **2022**, *13*, 377. [CrossRef]
47. Tsiourlis, G.; Konstantinidis, P.; Xofis, P. Syntaxonomy and Synecology of *Juniperus phoenicea* L. shrublands in Greece. *J. Environ. Prot. Ecol.* **2016**, *17*, 182–190.
48. Tsiourlis, G.; Konstantinidis, P.; Xofis, P. Taxonomy and ecology of phryganic communities with *Sarcopoterium spinosum* (L.) Spach of the Aegean (Greece). *Isr. J. Plant Sci.* **2007**, *55*, 15–34. [CrossRef]
49. Harris, I.; Osborn, T.J.; Jones, P.; Lister, D.H. Version 4 of the CRU TS monthly high-resolution gridded multivariate climate dataset. *Sci. Dara* **2020**, *7*, 109. [CrossRef] [PubMed]
50. Lagouvardos, K.; Kotroni, V.; Bezes, A.; Koletsis, I.; Kopania, T.; Lykoudis, S.; Mazarakis, N.; Papagiannaki, K.; Vougioukas, S. The automatic weather stations NOANN network of the National Observatory of Athens: Operation and database. *Geosci. Data J.* **2017**, *4*, 4–16. [CrossRef]
51. Du, L.; Tian, Q.; Yu, T.; Meng, Q.; Jancso, T.; Udvardy, P.; Huang, Y. A comprehensive drought monitoring method integrating MODIS and TRMM data. *Int. J. Appl. Earth Obs. Geoinf.* **2013**, *23*, 245–253. [CrossRef]
52. Liu, Q.; Zhang, S.; Zhang, H.R.; Bai, Y.; Zhang, J.H. Monitoring drought using composite drought indices based on remote sensing. *Sci. Total Environ.* **2020**, *711*, 134585. [CrossRef]
53. Tianyu, L.; Meng, Q. A mixture emissivity analysis method for urban land surface temperature retrieval from Landsat 8 data. *Landsc. Urban Plan.* **2018**, *179*, 63–71. [CrossRef]
54. Quiring, S.M.; Ganesh, S. Evaluating the utility of the Vegetation Condition Index (VCI) for monitoring meteorological drought in Texas. *Agric. For. Meteorol.* **2010**, *150*, 330–339. [CrossRef]
55. Yue, S.; Wang, C. The Mann-Kendall Test Modified by Effective Sample Size to Detect Trend in Serially Correlated Hydrological Series. *Water Resour. Manag.* **2004**, *18*, 201–218. [CrossRef]
56. Ali, E.; Cramer, W.; Carnicer, J.; Georgopoulou, E.; Hilmi, N.J.M.; Le Cozannet, G.; Lionello, P. Cross-Chapter Paper 4: Mediterranean Region. In *Climate Change 2022: Impacts, Adaptation and Vulnerability. Contribution of Working Group II to the Sixth Assessment Report of the Intergovernmental Panel on Climate Change*; Pörtner, H.-O., Roberts, D.C., Tignor, M., Poloczanska, E.S., Mintenbeck, K., Alegría, A., Craig, M., Langsdorf, S., Löschke, S., Möller, V., et al., Eds.; Cambridge University Press: New York, 2022; pp. 2233–2272.
57. Fernández-González, S.; Pereira, S.C.; Castro, A.; Rocha, A.; Fraile, R. Connection between autumn Sea Surface Temperature and winter precipitation in the Iberian Peninsula. *Glob. Planet. Change* **2014**, *121*, 9–18. [CrossRef]

58. Luppichini, M.; Bini, M.; Barsanti, M.; Giannecchini, R.; Zanchetta, G. Seasonal rainfall trends of a key Mediterranean area in relation to large-scale atmospheric circulation: How does current global change affect the rainfall regime? *J. Hydrol.* **2022**, *612*, 128233. [CrossRef]
59. Pastor, F.; Valiente, J.A.; Estrela, M.J. Sea surface temperature and torrential rains in the Valencia region: Modelling the role of recharge areas. *Nat. Hazards Earth Syst. Sci.* **2015**, *15*, 1677–1693. [CrossRef]
60. Pisano, A.; Marullo, S.; Artale, V.; Falcini, F.; Yang, C.; Leonelli, F.E.; Santoleri, R.; Buongiorno Nardelli, B. New Evidence of Mediterranean Climate Change and Variability from Sea Surface Temperature Observations. *Remote Sens.* **2020**, *12*, 132. [CrossRef]
61. Volosciuk, C.; Maraun, D.; Semenov, V.A.; Tilinina, N.; Gulev, S.K.; Latif, M. Rising Mediterranean Sea Surface Temperatures Amplify Extreme Summer Precipitation in Central Europe. *Sci. Rep.* **2016**, *6*, 32450. [CrossRef]
62. Pastor, F.; Valiente, J.A.; Khodayar, S. A Warming Mediterranean: 38 Years of Increasing Sea Surface Temperature. *Remote Sens.* **2020**, *12*, 2687. [CrossRef]
63. MacDonald, D.; Crabtree, J.R.; Wiesinger, G.; Dax, T.; Stamou, N.; Fleury, P.; Gutierrez Lazpita, J.; Gibon, A. Agricultural abandonment in mountain areas of Europe: Environmental consequences and policy response. *J. Environ. Manag.* **2000**, *59*, 47–69. [CrossRef]
64. Preiss, E.; Martin, J.-L.; Debussche, M. Rural depopulation and recent landscape changes in a Mediterranean region: Consequences to the breeding avifauna. *Landsc. Ecol.* **1997**, *12*, 288–296. [CrossRef]
65. Queiroz, C.; Beilin, R.; Folke, C.; Lindborg, R. Farmland abandonment: Threat or opportunity for biodiversity conservation? A global review. *Front. Ecol. Environ.* **2014**, *12*, 288–296. [CrossRef]
66. Xofis, P.; Poirazidis, K. Combining different spatio-temporal resolution images to depict landscape dynamics and guide wildlife management. *Biol. Conserv.* **2018**, *218*, 10–17. [CrossRef]
67. Founda, D.; Giannakopoulos, C. The exceptionally hot summer of 2007 in Athens, Greece—A typical summer in the future climate? *Glob. Planet. Change* **2009**, *67*, 227–236. [CrossRef]
68. Tolika, K.; Maheras, P.; Tegoulias, I. Extreme temperatures in Greece during 2007: Could this be a "return to the future"? *Gephysical Res. Lett.* **2009**, *36*, L10813. [CrossRef]
69. Nastos, P.T.; Kapsomenakis, J. Regional climate model simulations of extreme air temperature in Greece. Abnormal or common records in the future climate. *Atmos. Res.* **2015**, *152*, 43–60. [CrossRef]
70. Giannakopoulos, C.; Le Sager, P.; Bindi, M.; Moriondo, M.; Kostopoulou, E.; Goodess, C.M. Climatic Changes and Associated Impacts in the Mediterranean Resulting from a 2 °C Global Warming. *Glob. Planet. Change* **2009**, *68*, 209–224. [CrossRef]
71. Iglesias, A.; Garrote, L.; Flores, F.; Moneo, M. Challenges to Manage the Risk of Water Scarcity and Climate Change in the Mediterranean. *Water Resour. Manag.* **2007**, *21*, 775–788. [CrossRef]
72. López-Moreno, J.I.; Goyette, S.; Beniston, M. Climate Change Prediction over Complex Areas: Spatial Variability of Uncertainties and Predictions over the Pyrenees from a Set of Regional Climate Models. *Int. J. Climatol.* **2008**, *28*, 1535–1550. [CrossRef]
73. Feloni, E.; Nastos, P.T. Evaluating Rainwater Harvesting Systems for Water Scarcity Mitigation in Small Greek Islands under Climate Change. *Sustainability* **2024**, *16*, 2592. [CrossRef]
74. Hadjigeorgiou, P. Achieving Water Security—Cyprus Case. In Proceedings of the The Cyprus Institute Conference, Nicosia, 22nd March 2022. 2022. Available online: https://www.moa.gov.cy/moa/wdd/wdd.nsf/All/1FE8FD8BD5DD9E79C225880F0026DC54/$file/Achieving%20Water%20Security-Cyprus%20Case_Nicosia_2022.pdf (accessed on 23 November 2024).

Disclaimer/Publisher's Note: The statements, opinions and data contained in all publications are solely those of the individual author(s) and contributor(s) and not of MDPI and/or the editor(s). MDPI and/or the editor(s) disclaim responsibility for any injury to people or property resulting from any ideas, methods, instructions or products referred to in the content.